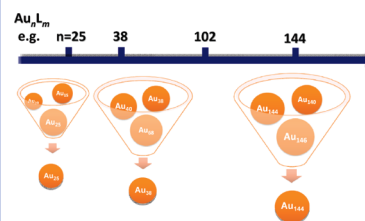


Size Focusing: A Methodology for Synthesizing Atomically Precise Gold Nanoclusters

Rongchao Jin,* Huifeng Qian, Zhikun Wu, Yan Zhu, Manzhou Zhu, Ashok Mohanty, and Niti Garg

Department of Chemistry, Carnegie Mellon University, Pittsburgh, Pennsylvania 15213

ABSTRACT Controlling nanoparticles with atomic precision, somewhat like the way organic chemists control small molecules by organic chemistry principles, is highly desirable for nanoparticle chemists. Recent advances in the synthesis of gold nanoparticles have opened the possibility to precisely control the number of gold atoms in a particle. In this Perspective, we will discuss a size-focusing methodology that has been developed in the synthesis of a number of atomically monodisperse ultrasmall gold nanoparticles (also called nanoclusters). We focus our discussion on thiolate-stabilized Au nanoclusters (referred to as $Au_n(SR)_m$, where n and m are the respective number of metal atoms and ligands). The underlying principle of this size-focusing process is primarily related to the peculiar stability of certain sized $Au_n(SR)_m$ nanoparticle, that is, “survival of the robustest”, much like the natural law “survival of the fittest”. We expect that this universal size-focusing method will ultimately allow for preparing a full series of size-discrete, atomically monodisperse nanoparticles that span the size regimes of both nonplasmonic nanoclusters and plasmonic nanocrystals. These well-defined nanoparticles will be of major importance for both fundamental science research and technological applications.



To control nanoparticles with atomic precision has long been a major dream of nanoparticle chemists. Such an atomic level of synthetic control is quite routine in molecular chemistry but poses a major challenge in nanoparticle chemistry. Nevertheless, recent advances have opened up the possibility of preparing atomically precise nanoparticles, at least in the ultrasmall size regime, and a number of well-defined gold nanoparticles with precise formulas (referred to as $Au_n L_m$, where L is typically thiolate) have been achieved.^{1–7}

Noble metal nanoparticles, especially gold, have a long history of scientific studies. The earliest scientific work by Faraday on the preparation of gold colloids dates back to 1857,⁸ and this work stimulated tremendous interests in this new form of gold,^{9,10} in particular, about the origin of the beautiful ruby red color of colloidal gold. It is worth noting that the distinct color of gold had long been utilized in colorful decoration, even in ancient times (e.g., a few thousand years ago), much earlier than the 19th century's scientific studies on gold colloids, but ancient practitioners certainly had not realized that the attractive ruby color of gold is indeed due to its nanoscale form. Since Faraday's original work, Mie was the first who successfully modeled the optical spectra of gold colloids by solving Maxwell's equations in 1908.¹⁰ However, the physical nature of the absorption and scattering properties of nanoparticles still remained unclear for a long time. It was not until the full establishment of the electronic band theory of metals during the 1950–60s, a new concept of plasma and its excitation mode, plasmon, which was originally developed by Langmuir in gas-phase research, were

then introduced into metal nanoparticles.¹¹ The exact nature of the unique color of gold nanoparticles was finally understood. Nowadays, it is well-known that the plasmon excitation is a collective excitation of conduction electrons in a metal particle when light is incident on the particle. This collective mode is in striking contrast with the single electron excitation mode in small molecules.

Starting in the 1940s, the transmission electron microscope (TEM) began to be utilized in nanoparticle research;¹² it allowed, for the first time, physical seeing of nanoparticle morphology and precise measurement of particle size, rather than indirect “seeing” of nanoparticles by the dark-field Tyndall (or scattering) effect using an optical ultramicroscope.¹³ With the popularization of TEM in the 1960–70s, an intriguing phenomenon, multiple twinning in vacuum-deposited Au nanoparticles, was observed and studied in detail.^{14,15} Solution-phase synthesis of Au nanoparticles with a narrow size distribution was also attained to some extent.^{16,17}

The emergence of nanoscience and nanotechnology in the late 1980s significantly boosted scientific research on metal nanoparticles as well as other major types such as quantum dots and magnetic nanoparticles. Gold nanoparticles possess particular chemical stability and have drawn significant interests in current nanoscience and nanotechnology research.¹⁸

Received Date: July 12, 2010

Accepted Date: September 10, 2010

In early work, colloidal Au nanoparticles were stabilized by surface-adsorbed simple ions (e.g., Cl^- , OH^-), small molecules (e.g., citrate), or polymers (e.g., starch). These nanoparticles are not stable enough and can only exist in solution format; upon being dried, these particles aggregate irreversibly and can no longer be redispersed. Starting in the late 1980s, intense research on the self-assembled monolayer (SAM) of thiols on bulk gold surfaces was carried out.¹⁹ The covalent Au–S bond was found to be particularly robust in SAMs. The SAM research apparently inspired many researchers to use thiol to stabilize gold nanoparticles.^{20–23} Tremendous research has since then been carried out on thiolate-stabilized gold nanoparticles.¹

For metal nanoparticles (typically ranging from ~ 1 to 100 nm), there are two interesting size regimes, (I) from sub-nanometer to ~ 2 nm and (II) from ~ 2 to ~ 100 nm. Metal nanoparticles in regime II are plasmonic, and they show strong plasmon resonance(s) in the optical absorption and scattering spectra, which has been well-studied in the past decades. In contrast, particles in size regime I exhibit many interesting quantum confinement effects, such as the disappearance of plasmon resonance and emergence of a molecular-like HOMO–LUMO transition.^{1,24–29} Here, we focus on gold nanoparticles in size regime I. If one counts the number of metal atoms per particle (Au_nL_m), the size range of 1–2 nm is roughly equivalent to a range of n from ~ 10 to ~ 250 atoms. Note that the number of Au atoms per particle can be estimated by a simple relation, $n = (\text{particle volume, nm}^3) \times 59 \text{ atoms/nm}^3$. This equation is derived from fcc (face-centered cubic) gold, but it provides an accurate enough estimation even for non-fcc-structured Au nanoclusters in regime I (smaller than 2 nm);¹ this is justified by their similar atomic packing density in both size regimes. With respect to experimental control over the number of atoms in $\text{Au}_n(\text{SR})_m$ nanoparticles, it was a major challenge to chemists but has recently become possible, at least to some extent.¹

To obtain atomically precise nanoparticles (e.g., gold, silver) is of paramount importance in order to determine their total structure (core and surface atomic arrangements) and to understand the fundamental science of nanoparticles.

In this Perspective, we will discuss recent important advances in synthesizing atomically precise gold nanoparticles. The currently reported works primarily focus on ultrasmall gold thiolate nanoparticles (< 2 nm); these small particles are also called nanoclusters since they often adopt non-fcc structures and their electronic structures are significantly different from that of plasmonic Au nanocrystals and are drastically affected by the atom packing structure and

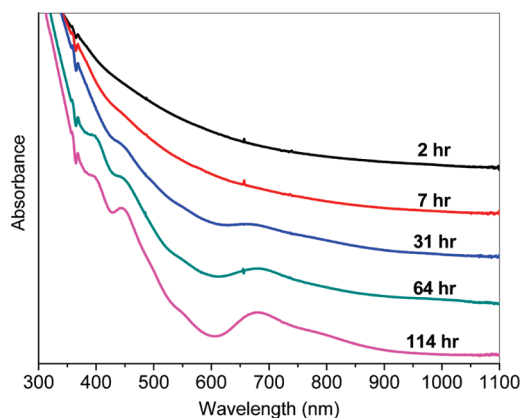


Figure 1. Evolution of the UV–vis spectra of the crude product with aging time (at room temperature). The spectra are vertically shifted for the ease of comparison.

quantum confinement effects. We will introduce a “size-focusing” methodology for synthesizing atomically precise gold nanoparticles. With this method, a number of well-defined gold nanoclusters have been made. This method has also been extended to silver nanoclusters.

Case of $\text{Au}_{25}(\text{SR})_{18}$. We first noticed the size-focusing phenomenon in our early work on the synthesis of $\text{Au}_{25}(\text{SR})_{18}$ nanoclusters (abbreviated as Au_{25} below).^{4,30} Our two-phase⁴ and one-phase³⁰ synthetic methods are modifications of previous works reported by Whetten, Murray, and Tsukuda et al. for synthesizing ultrasmall $\text{Au}_n(\text{SR})_m$ nanoparticles.^{25–27,31} In our syntheses of Au_{25} in both systems, the first step, reduction of Au(III) by excess thiol to form a Au(I)/SR polymeric intermediate, was done at a low temperature (e.g., 0°C) rather than at room temperature, as commonly done by other researchers. This is indeed a critical step for high-yield synthesis of Au_{25} with high purity.^{4,30} We noticed that, following the reduction of Au(I)/SR by NaBH_4 at 0°C , several prominent peaks in the UV–vis spectrum of the crude product emerged after prolonged aging of the reaction product, while the Au(I) intermediate formed at room temperature did not lead to monodisperse Au_{25} .⁴ A detailed investigation into this aging process revealed a gradual growth of monodisperse Au_{25} nanoparticles from the size-mixed product, Figure 1. Three absorption peaks at 670, 450, and 400 nm were observed,³⁰ which are characteristic of $\text{Au}_{25}(\text{SR})_{18}$ nanoparticles and can thus be conveniently used to identify/trace the growth process.

This size-focusing growth process was found to be quite common (e.g., not limited by the type of thiol). In all $\text{Au}_{25}(\text{SR})_{18}$ with long-chain or aromatic thiols investigated in our work³⁰ (where, $\text{R} = -\text{C}_2\text{H}_4\text{Ph}$, $-\text{C}_6\text{H}_{13}$, $-\text{C}_{12}\text{H}_{25}$, $-\text{G}$ (glutathione), $-\text{n-C}_{10}\text{H}_{22}\text{COOH}$, etc), a universal size-focusing process was found. Recently, Dass and co-workers reported matrix-assisted laser desorption ionization (MALDI) mass spectrometric evidence for the size-focusing growth process of Au_{25} in one-phase synthesis.³² They observed that at earlier reaction times, a mixture ranging from Au_{25} to Au_{102} was formed, and subsequently, size evolution led to highly monodisperse Au_{25} (Figure 2).

With respect to nanocluster characterization, it is worth noting that MALDI-MS often results in fragmentation of nanoclusters,

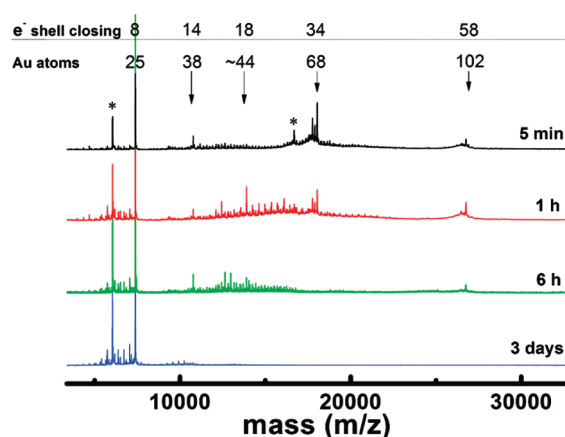


Figure 2. Mass spectrometric evidence of size focusing in the one-phase synthesis of $\text{Au}_{25}(\text{SC}_2\text{H}_4\text{Ph})_{18}$ nanoparticles. MALDI matrix: DCTB (*trans*-2-[3-(4-*tert*-butylphenyl)-2-methyl-2-propenyldiene] malononitrile), operated at the threshold laser fluence. Peaks marked by asterisks are fragments. Adapted from ref 32.

even under threshold laser intensity; thus, electrospray ionization mass spectrometry (ESI-MS) is indispensable for nanocluster characterization and is indeed critical for unequivocal determination of cluster formula. Compared to MALDI-MS, ESI-MS is a much softer ionization technique and usually does not result in fragmentation of nanoparticles. A representative ESI mass spectrum of $\text{Au}_{25}(\text{SC}_2\text{H}_4\text{Ph})_{18}^-$ is shown in Figure 3A.^{33,34} For small nanoclusters such as Au_{25} , TEM is not very informative (Figure 3B); one can barely see the nanoparticles. Although TEM can confirm that the particles are small (e.g., < 2 nm), it is not possible to determine the exact number of gold atoms in the particle. High-resolution TEM based upon phase contrast is not useful either because small $\text{Au}_n(\text{SR})_m$ nanoclusters are not fcc crystalline (i.e., no translational symmetry).

An important question pertains to what drives the size-focusing process. On the basis of the current knowledge, this seems closely related to the stability of different sized $\text{Au}_n(\text{SR})_m$ nanoclusters. The initial product (prior to aging or spontaneous size focusing) shows a decaying optical spectrum, typically implying a mixture (Figure 1, see the 2 h spectrum), also demonstrated by Dass et al. in MS characterization.³² A similar featureless spectrum had also been observed earlier in the $\text{Au}_n(\text{SG})_m$ system.²⁶ Tsukuda and co-workers performed an elegant electrophoresis separation of the mixture and attained a number of glutathione-capped $\text{Au}_n(\text{SG})_m$ clusters, including $\text{Au}_{10}(\text{SG})_{10}$, $\text{Au}_{15}(\text{SG})_{13}$, $\text{Au}_{18}(\text{SG})_{14}$, $\text{Au}_{22}(\text{SG})_{16}$, $\text{Au}_{22}(\text{SG})_{17}$, $\text{Au}_{25}(\text{SG})_{18}$, $\text{Au}_{29}(\text{SG})_{20}$, $\text{Au}_{33}(\text{SG})_{22}$, and $\text{Au}_{39}(\text{SG})_{24}$.^{26,35} They further observed that all of the sizes with $n < 25$ were decomposed upon etching with excess thiol (G-SH), but Au_{25} was found to be stable.³⁶ Pradeep and co-workers obtained monodisperse $\text{Au}_{25}(\text{SG})_{18}$ nanoclusters by etching the crude product (a mixture of $\text{Au}_n(\text{SG})_m$) using excess GSH.^{5,37} When retrospectively the earlier size-focusing synthesis of $\text{Au}_{25}(\text{SR})_{18}$, we deem that the mechanism should be as follows; upon NaBH_4 reduction of the peculiar $\text{Au}(\text{I})/\text{SR}$ polymeric intermediate (formed at low temperature), a number of sizes are concurrently produced, but these

different sized nanoparticles are, however, vastly different in stability, which leads to a spontaneous size-focusing process during the aging process, and ultimately only the robustest size survives the size-focusing process. By carefully controlling the reaction conditions, we obtain highly pure $\text{Au}_{25}(\text{SR})_{18}$ nanoparticles, which leads to successful crystallization and X-ray structure determination of this nanoparticle.^{28,29}

The size-focusing synthesis of $\text{Au}_{25}(\text{SR})_{18}$ nanoparticles implies a principle of “survival of the robustest”, much like the natural law “survival of the fittest”.

The case of Au_{25} synthesis has illustrated the basic principle of the size-focusing growth process, which is based upon the stability property of different sized nanoclusters. In order to attain atomic monodispersity, only one size of nanoparticles should survive the size-focusing process, but sometimes, multiple sizes (with comparable stability) might result; that is why earlier syntheses of $\text{Au}_n(\text{SR})_m$ could not produce atomically monodisperse nanoparticles. An important issue is how to render just one size to survive the focusing process. In our subsequent work, we found that it is critical to control the starting $\text{Au}_n(\text{SR})_m$ mixture's size distribution. Below, we shall elaborate on this size-focusing methodology with more examples, including the syntheses of $\text{Au}_{38}(\text{SR})_{24}$ and $\text{Au}_{144}(\text{SR})_{60}$ nanoparticles with molecular purity.

Case of $\text{Au}_{38}(\text{SR})_{24}$. The Au_{38} nanoparticles pertain to the ~ 8 kDa species earlier reported by Whetten and co-workers.^{25,38} Toikkanen et al. isolated a relevant species and determined its formula to be $\text{Au}_{38}(\text{SC}_6\text{H}_{13})_{22}$ by MALDI-MS.³⁹ Recently, Chaki et al. reported the isolation of 38-gold-atom nanoparticles capped by dodecanethiolate and unequivocally determined the formula to be $\text{Au}_{38}(\text{SC}_{12}\text{H}_{25})_{24}$ by ESI-MS analysis,⁴⁰ but its yield was quite low.

Qian et al. improved the Au_{38} synthetic method and were able to increase the yield of $\text{Au}_{38}(\text{SC}_{12}\text{H}_{25})_{24}$ to $\sim 10\%$ via a two-step approach, and the $\text{Au}_{38}(\text{SC}_{12}\text{H}_{25})_{24}$ composition was verified by ESI-MS and other characterization.⁴¹ In this method, a crude mixture of glutathione-capped $\text{Au}_n(\text{SG})_m$ nanoparticles was first made; the mixed nanoparticles were then subjected to a thermal thiol etching process in a two-phase (water/organic) system; note that size focusing occurs in the thermal etching step. After the ligand exchange (from $-\text{SG}$ to $-\text{SC}_{12}\text{H}_{25}$) on the $\text{Au}_n(\text{SG})_m$ nanoparticles was completed, the subsequent etching process (in neat dodecanethiol) caused gold core etching, and eventually, the starting polydisperse nanoparticles were converted to monodisperse $\text{Au}_{38}(\text{SC}_{12}\text{H}_{25})_{24}$ with high purity. This size-focusing synthesis is advantageous over earlier work as it eliminates nontrivial postsynthetic separation steps.⁴⁰

Recently, Qian et al. have extended the two-step method to the synthesis of phenylethylthiolate-capped $\text{Au}_{38}(\text{SC}_2\text{H}_4\text{Ph})_{24}$ and attained a yield of $\sim 25\%$ (Au atom basis) after optimization

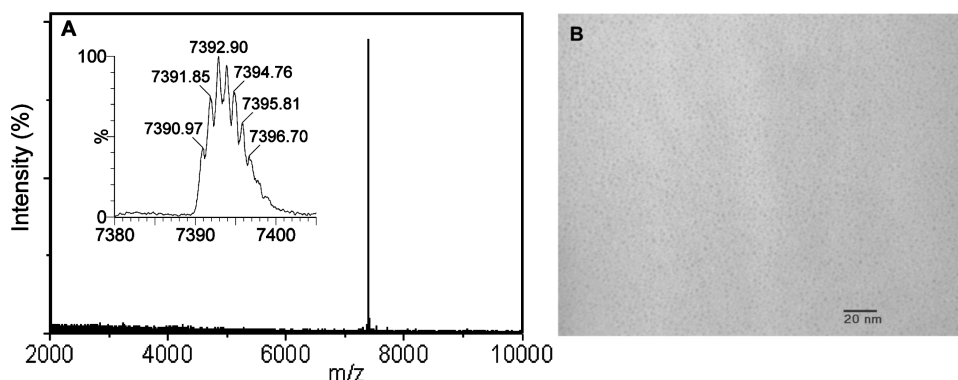


Figure 3. (A) ESI-MS characterization (negative mode) of $\text{Au}_{25}(\text{SC}_2\text{H}_4\text{Ph})_{18}^-$ nanoclusters (counterion: tetraoctylammonium, TOA^+); the inset shows the isotope pattern, which allows for the determination of the charge state (in this case, $z = 1$). (B) TEM image of the Au_{25} particles. Adapted from ref 33.

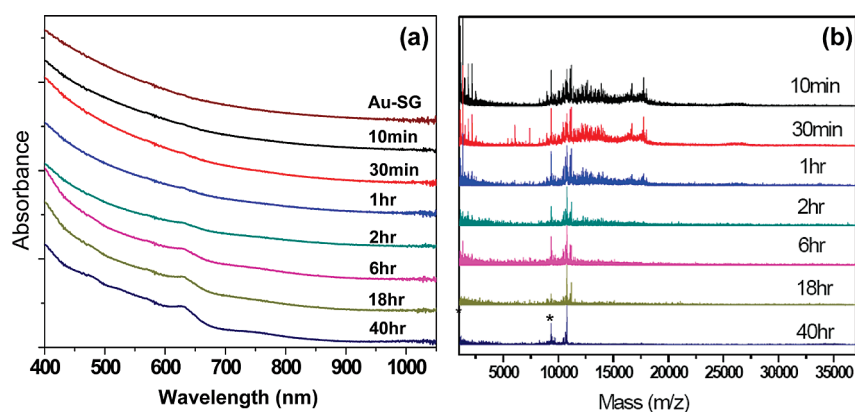


Figure 4. Temporal evolution of UV-vis spectra (a) and MALDI mass spectra (b) of Au nanoparticles during the size-focusing reaction. Au-SG stands for the starting $\text{Au}_n(\text{SG})_m$ mixture in aqueous solution. 10 min–40 h indicates the time that $\text{Au}_n(\text{SG})_m$ reacts with excess $\text{PhC}_2\text{H}_4\text{SH}$. The asterisk shows a fragment of $\text{Au}_{38}(\text{SC}_2\text{H}_4\text{Ph})_{24}$. Adapted from ref 42.

of some reaction parameters;⁴² note that $\sim 75\%$ gold was lost as $\text{Au}(\text{I})/\text{SR}$ complexes as well as in various synthetic steps. The $\text{Au}_{38}(\text{SC}_2\text{H}_4\text{Ph})_{24}$ nanoclusters were readily separated from excess thiols by precipitating the clusters (together with $\text{Au}(\text{I})/\text{SR}$ polymeric complexes) with copious ethanol, followed by extraction with toluene for $\text{Au}_{38}(\text{SC}_2\text{H}_4\text{Ph})_{24}$; note that $\text{Au}(\text{I})/\text{SR}$ polymeric complexes were left in the residues because they are not soluble in toluene. A detailed mechanistic investigation on the conversion process clearly shows a size-focusing process, evidenced by both optical spectroscopy and MALDI-MS analyses (Figure 4). The optical spectrum of the starting $\text{Au}_n(\text{SC}_2\text{H}_4\text{Ph})_m$ shows a decaying curve, indicating a mixture; with reaction going on, several distinct peaks start to emerge in the spectrum, and the final product shows a distinctive optical spectrum characteristic of Au_{38} nanoparticles (Figure 4a).^{40,41} MALDI-MS analysis reveals that with the increase of reaction time, the relatively large Au nanoparticles ($n > 38$) seem to decompose and convert to Au_{38} (Figure 4b). After ~ 40 h, very clean $\text{Au}_{38}(\text{SC}_2\text{H}_4\text{Ph})_{24}$ nanoparticles (10780 Da, $z = 1$) were obtained (Figure 4b); note that a fragment (9342 Da, $z = 1$) of the Au_{38} nanoparticle was also seen, while in ESI-MS analysis (Figure 5), this fragment was not observed.⁴²

As discussed above, a key condition to obtain one size of nanoparticles is to control the size distribution of the $\text{Au}_n(\text{SG})_m$ mixture prior to the size-focusing step. We realized that the solvent might play an important role in controlling the size range of the $\text{Au}_n(\text{SG})_m$ starting mixture.⁴² Prior to our work, the $\text{Au}_n(\text{SG})_m$ nanoparticles were typically prepared in methanol.^{26,30,31,37} Guided by the size-focusing principle, we modified the synthetic procedure by replacing methanol with other solvents and found that acetone is indeed a good solvent for high-yielding synthesis of $\text{Au}_{38}(\text{SR})_{24}$ nanoparticles as methanol gives rise to a proper size distribution of $\text{Au}_n(\text{SG})_m$ as the starting material for the size-focusing step. Figure 6 shows the different size distributions of the $\text{Au}_n(\text{SG})_m$ mixture synthesized in methanol and acetone. The acetone-mediated synthesis of $\text{Au}_n(\text{SG})_m$ nanoparticles produces a dominant size range from 8 to 18 kDa ($z = 1$), while the methanol system produces a dominant size range below 8 kDa. Regarding the specific role(s) of the solvent, we believe that the solvent influences the $[\text{Au}(\text{I})/\text{SR}]_x$ aggregate size and/or structure, which subsequently affects the cluster sizes, but details remain to be elucidated. We attribute the high yield of $\text{Au}_{38}(\text{SC}_2\text{H}_4\text{Ph})_{24}$ to the down conversion of those higher-mass $\text{Au}_n(\text{SG})_m$ nanoparticles ($38 < n \leq 102$). For the starting nanoparticles

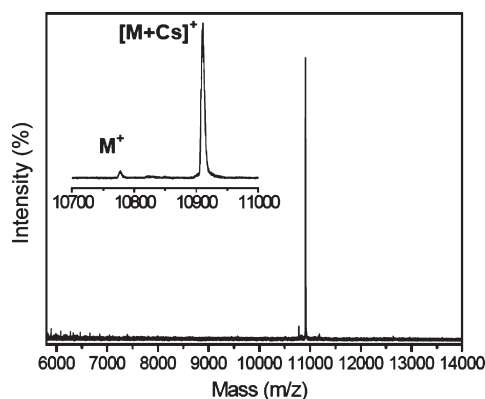


Figure 5. ESI-MS characterization (positive mode) of neutral $\text{Au}_{38}(\text{SC}_2\text{H}_4\text{Ph})_{24}$ nanoclusters. To promote particle ionization, CsOAc was added. The signal at m/z 10777.5 ($z = 1$, assigned to M^+) is due to spontaneous ionization under ESI conditions; this signal is minor compared to that of the $[\text{M}-\text{Cs}]^+$ adduct (M stands for the particle). Adapted from ref 42.

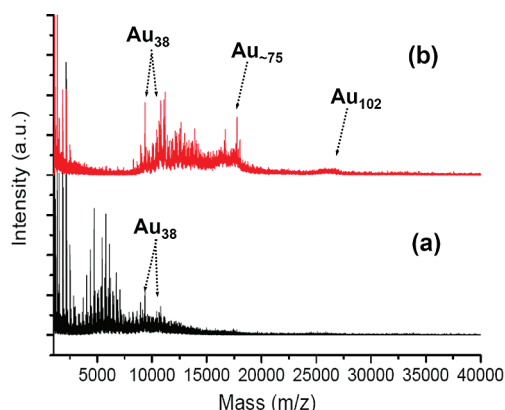


Figure 6. MALDI mass spectra of Au nanoparticles obtained from ligand exchange of $\text{Au}_n(\text{SG})_m$ with $\text{PhC}_2\text{H}_4\text{SH}$ (reaction for 10 min). The starting $\text{Au}_n(\text{SG})_m$ nanoparticles were made (a) in methanol and (b) in acetone. Adapted from ref 42.

made in methanol, the final Au_{38} yield was low because the majority of the starting $\text{Au}_n(\text{SG})_m$ nanoparticles were smaller than 38 atoms (Figure 6a). Thus, it is important to prepare somewhat larger Au_n nanoparticles with $n > 38$ but not too large, so that these appropriate nanoparticles can be readily converted to Au_{38} .⁴² Note that we did not observe upconversion of smaller ones ($n < 38$, such as Au_{25}) into Au_{38} , which is in contrast with previously reported conversion of Au_{11} phosphine clusters into $\text{Au}_{25}(\text{SG})_{18}$.² In the thiol etching process, O_2 is most probably involved in crashing those less-stable clusters, but a detailed mechanism remains to be unraveled in future work. The high-yielding synthesis has led to the crystallization and structure determination of $\text{Au}_{38}(\text{SR})_{24}$.⁴³

Case of $\text{Au}_{144}(\text{SR})_{60}$. The size-focusing methodology has also been employed to synthesize atomically monodisperse Au_{144} nanoparticles. It is noteworthy that a relevant 29 kDa species (assigned to $\text{Au}_{140-146}(\text{SR})_{50-60}$) was previously reported by Schaaff et al.^{25,44} and Hicks et al.⁴⁵ Chaki et al.

recently reported a $\text{Au}_{144}(\text{SC}_{12}\text{H}_{25})_{59}$ species.⁴⁰ The formula of $\text{Au}_{144}(\text{SR})_{60}$ was suggested by Lopez-Acevedo et al. in their theoretical work⁴⁶ and confirmed by ESI-MS analyses by Qian et al.⁴⁷ and Fields-Zinna et al.⁴⁸

We devised a two-step approach to synthesizing monodisperse $\text{Au}_{144}(\text{SC}_2\text{H}_4\text{Ph})_{60}$ nanoparticles. In the first step, polydisperse Au nanoparticles capped by $-\text{SC}_2\text{H}_4\text{Ph}$ thiolate were made by NaBH_4 reduction of $\text{Au}(\text{I})/\text{SR}$ intermediates.⁴⁷ Again, it is important to control the size range of the $\text{Au}_n(\text{SC}_2\text{H}_4\text{Ph})_m$ mixture. One should control the size range to be above Au_{38} ; otherwise, both Au_{144} and Au_{38} may result after size focusing. By adjusting the experimental conditions,⁴⁷ such as the thiol/Au ratio ($\sim 3\times$ used), reaction temperature and kinetic control, one can obtain appropriately size-distributed Au nanoparticles (< 2 nm) as the starting material for size-focusing synthesis of Au_{144} . MALDI-MS analysis showed a dominant size range from ~ 24 to 36 kDa ($z = 1$) (Figure 7); note that the peak at 7394 Da ($z = 1$) is from $\text{Au}_{25}(\text{SC}_2\text{H}_4\text{Ph})_{18}$, and the 6058 Da ($z = 1$) peak is a fragment of Au_{25} , assigned to $\text{Au}_{21}(\text{SC}_2\text{H}_4\text{Ph})_{14}$. These polydisperse nanoparticles were used as the precursor for the size-focusing step. In the presence of excess $\text{PhCH}_2\text{CH}_2\text{SH}$ and at 80 °C, the polydisperse Au nanoparticles were gradually converted to monodisperse Au_{144} within ~ 24 h. Note that the MALDI-MS peak of monodisperse Au_{144} product was broadened for some reason (Figure 7A), but ESI-MS confirms that the as-prepared nanoparticles were indeed truly monodisperse (Figure 7C). Two sets of peaks corresponding to Cs adducts of Au_{144} were observed in ESI-MS.⁴⁷ The UV-vis absorption spectrum of the initial Au nanoparticles (prior to thiol etching) shows an essentially featureless curve spanning the entire UV-vis spectrum [Figure 7B (black profile)], which implies polydisperse nanoparticles prior to size focusing, but after size focusing, the final Au_{144} nanoparticles show prominent absorption bands at ~ 510 (2.44 eV) and ~ 700 nm (1.78 eV) in the 300–1100 nm range.⁴⁷

Nature produces every size of nanoparticles, but these different sized nanoparticles are vastly different in terms of stability, which forms the basis of the size-focusing methodology.

Summary. This size-focusing methodology is interesting and should be extendable to the synthesis of other stable $\text{Au}_n(\text{SR})_m$ nanoparticles. As previously discussed, the basis of the methodology is the stability property of different sized $\text{Au}_n(\text{SR})_m$ nanoparticles, which allows one to use appropriate conditions (e.g., aging or thermal thiol etching) to selectively crash those less-stable particles in the size distribution but permit the most robust one to survive the focusing process. This raises a fundamental question, what determines the particle stability, electronic, geometric, or other factors? We

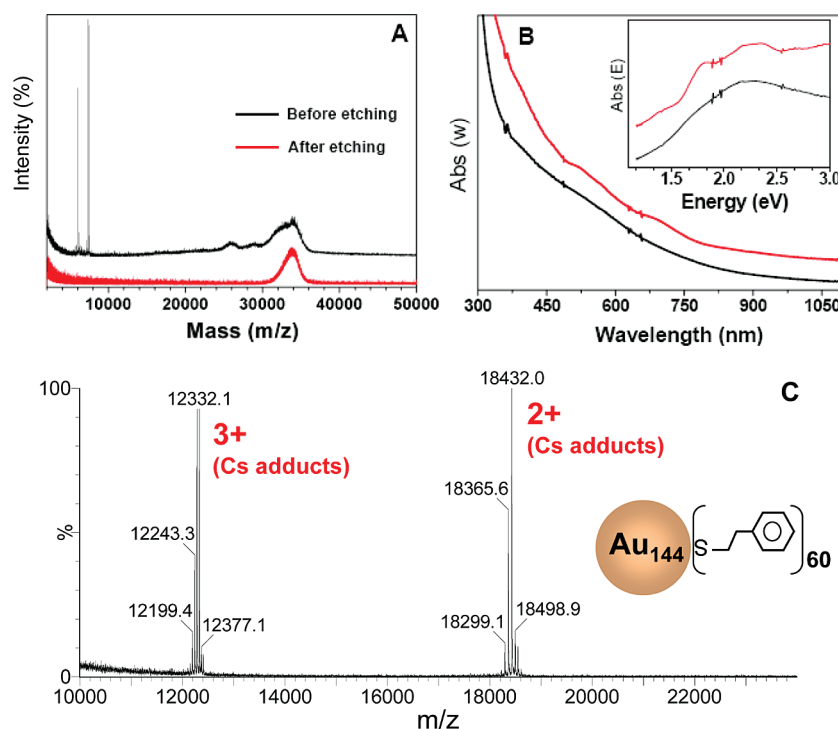


Figure 7. (A) MALDI mass spectra of Au nanoparticles before (black profile) and after thiol etching (red profile). (B) UV-vis absorption spectra of Au nanoparticles before (black profile) and after thiol etching (red profile). Inset: optical absorbance versus photon energy (eV). The spectra are shifted for the ease of comparison. (C) ESI-MS spectrum of the final Au₁₄₄(SC₂H₄Ph)₆₀ nanoparticles. Adapted from ref 47.

have not fully understood this major issue. Detailed mechanistic studies are still needed to understand the size evolution process.^{49,50} It is worth mentioning that we also observed a size-focusing process in the synthesis of silver nanoparticles stabilized by thiolates.⁵¹ It remains to develop detailed protocols for other size and composition nanoclusters using the size focusing principle.^{52–56}

Two key points of the size-focusing methodology are (1) to utilize the different stability of different sized Au_n(SR)_m nanoparticles and (2) to have a proper size distribution of the starting Au_n(SR)_m mixture for size focusing down to one size.

In all cases (e.g., Au₂₅, Au₃₈, and Au₁₄₄), a key condition is to control the size distribution of the starting size-mixed nanoparticles (prior to the size-focusing step). A too broad size distribution would result in two or more robust nanoparticles after size-focusing, for instance, Au₃₈ and Au₁₄₄ with comparable stability may result from a broad 5–40 kDa Au_n(SR)_m starting material; isolation of them would be very difficult. Thus, in an ideal synthesis, one should control the

initial size distribution and render it favorable for size focusing down to one size. To achieve that, systematic investigation on the reaction parameters (e.g., reaction temperature, growth kinetics, ligand bulkiness, etching time, thiol/gold ratio, etc.) is still needed in future work. After mapping out those important parameters that affect the size distribution of nanoparticles and understanding more details of the size-focusing mechanism (e.g., down conversion or up conversion), one will ultimately be able to choose appropriate conditions for size-focusing synthesis of a specific size of nanoparticles. We expect that by exploring this size-focusing methodology, a series of size-discrete nanoparticles may be synthesized in future work, which will form the important basis for fundamental science research on the evolution of their structural, electronic, and optical properties with size.

AUTHOR INFORMATION

Corresponding Author:

*To whom correspondence should be addressed. E-mail: rongchao@andrew.cmu.edu.

Biographies

Rongchao Jin is an Assistant Professor of Chemistry at Carnegie Mellon University. He received his B.S. in Chemical Physics from the University of Science and Technology of China (Hefei, China) in 1995, M.S. in Physical Chemistry/Catalysis from Dalian Institute of Chemical Physics (Dalian, China) in 1998, and Ph.D. in Chemistry from Northwestern University (Evanston, Illinois) in 2003. After 3 years of postdoctoral research at the University of Chicago (Illinois), he joined the chemistry faculty of Carnegie Mellon University in

September, 2006. His current research interests focus on atomically precise noble metal nanoparticles, evolution of their structure, electronic and optical properties, and utilizing these well-defined nanoparticles in catalysis, optics, sensing, and so forth.

Huifeng Qian is a graduate student in the Jin group at Carnegie Mellon University. He obtained his B.S. in Chemistry (2004) and M.S. in Materials Science (2007) from Shanghai Jiao Tong University (Shanghai, China). His research interests are semiconductor quantum dots and noble metal nanoparticles.

Dr. Zhikun Wu is a postdoctoral researcher in the Jin group at CMU. He obtained his Ph.D. from the Institute of Chemistry, Chinese Academy of Sciences. His research interests are nanoparticles and molecular materials.

Dr. Yan Zhu is a postdoctoral researcher in the Jin group. She received her Ph.D. in Physical Chemistry from Nanjing University in 2007. Before joining the Jin group, she had worked at Keio University, where she worked on biomimetic membranes. Her current research interest is nanocatalysis.

Dr. Manzhou Zhu was a postdoctoral researcher in the Jin group and is now a Professor of Chemistry at Anhui University (China). He received his Ph.D. in Chemistry from the University of Science and Technology of China in 2000. Before joining the Jin group in February 2007, he worked at the University of Science and Technology of China. His research interests focus on photoinduced electron transfer, sensors, and nanomaterials.

Dr. Ashok Kumar Mohanty was a Visiting Scholar in the Jin group and now works at the National Metallurgical Laboratory (CSIR), Jamshedpur, India. He received his Ph.D. in Chemistry from the Indian Institute of Technology (Kharagpur) in 2005. His research interests are the design and synthesis of special types of surfactants and their use in nanoparticle synthesis.

Niti Garg is a graduate student in the Jin group at Carnegie Mellon University. She received her B.S. from St. Stephens College/Delhi University (Delhi) in 2003 and M.S. from the Indian Institute of Technology (Delhi) in 2005. Her thesis research focuses on controlled synthesis of noble metal nanoparticles and applications in chemical sensing and catalysis.

ACKNOWLEDGMENT We acknowledge financial support of our research by CMU, AFOSR, and NIOSH.

REFERENCES

- Jin, R. Quantum Sized, Thiolate-Protected Gold Nanoclusters. *Nanoscale* **2010**, *2*, 343–362.
- Shichibu, Y.; Negishi, Y.; Tsukuda, T.; Teranishi, T. Large-Scale Synthesis of Thiolated Au₂₅ Clusters via Ligand Exchange Reactions of Phosphine-Stabilized Au₁₁ Clusters. *J. Am. Chem. Soc.* **2005**, *127*, 13464–13465.
- Heaven, M. W.; Dass, A.; White, P. S.; Holt, K. M.; Murray, R. W. Crystal Structure of the Gold Nanoparticle [N(C₈H₁₇)₄][Au₂₅-(SCH₂CH₂Ph)₁₈]. *J. Am. Chem. Soc.* **2008**, *130*, 3754–3755.
- Zhu, M.; Lanni, E.; Garg, N.; Bier, M. E.; Jin, R. Kinetically Controlled, High-Yield Synthesis of Au₂₅ Clusters. *J. Am. Chem. Soc.* **2008**, *130*, 1138–1139.
- Shibu, E. S.; Habeeb Muhammed, M. A.; Tsukuda, T.; Pradeep, T. Ligand Exchange of Au₂₅SG₁₈ Leading to Functionalized Gold Clusters: Spectroscopy, Kinetics, and Luminescence. *J. Phys. Chem. C* **2008**, *112*, 12168–12176.
- Zhu, M.; Qian, H.; Jin, R. Thiolate-Capped Au₂₀ Clusters with a Large Energy Gap of 2.1 eV. *J. Am. Chem. Soc.* **2009**, *131*, 7220–7021.
- Zhu, M.; Qian, H.; Jin, R. Thiolate-Protected Au₂₄(SC₂H₄Ph)₂₀ Nanoclusters: Superatoms or Not? *J. Phys. Chem. Lett.* **2010**, *1*, 1003–1007.
- Faraday, M. Experimental Relations of Gold (and other Metals) to Light. *Philos. Trans. R. Soc. London* **1857**, *147*, 145–181.
- Zsigmondy, R. Amicroscopic Gold Germs. I. *Z. Phys. Chem.* **1906**, *56*, 65–76.
- Mie, G. Beiträge zur Optik Trüber Medien, Speziell Kolloidaler Metallösungen. *Ann. Phys.* **1908**, *25*, 377.
- Kreibig, U.; Vollmer, M. *Optical Properties of Metal Clusters*; Springer-Verlag: New York, 1995.
- Turkevich, J.; Hillier, J. Electron Microscopy of Colloidal Systems. *Anal. Chem.* **1949**, *21*, 475–485.
- Zsigmondy, R. Nobel Lecture *Properties of Colloids*, Nobel Lecture; Nobel Foundation, http://nobelprize.org/nobel_prizes/chemistry/laureates/1925/zsigmondy-lecture.pdf (December 11, 1926).
- Ogawaa, S.; Ino, S. Formation of Multiply-Twinned Particles in the Nucleation Stage of Film Growth. *J. Vac. Sci. Technol.* **1969**, *6*, 527–534.
- Marks, L. D. Imaging Small Particles. *Ultramicroscopy* **1985**, *18*, 445–452.
- Turkevich, J.; Stevenson, P. C.; Hillier, J. A Study of the Nucleation and Growth Processes in the Synthesis of Colloidal Gold. *Discuss. Faraday Soc.* **1951**, *11*, 55–75.
- Frens, G. Controlled Nucleation for the Regulation of the Particle Size in Monodisperse Gold Suspensions. *Nat. Phys. Sci.* **1973**, *241*, 20–22.
- Schmid, G., Ed. *Clusters and Colloids*; VCH: Weinheim, Germany, 1994.
- Colin, D. B.; George, M. W. Modeling Organic Surfaces with Self-Assembled Monolayers. *Angew. Chem., Int. Ed. Engl.* **1989**, *28*, 506–512.
- Brust, M.; Walker, M.; Bethell, D.; Schiffrin, D. J.; Whyman, R. Synthesis of Thiol-Derivatized Gold Nanoparticles in a Two-Phase Liquid-Liquid System. *J. Chem. Soc., Chem. Commun.* **1994**, 801–802.
- Mirkin, C. A.; Letsinger, R. L.; Mucic, R. C.; Storhoff, J. J. A DNA-Based Method for Rationally Assembling Nanoparticles into Macroscopic Materials. *Nature* **1996**, *382*, 607–609.
- Whetten, R. L.; Khoury, J. T.; Alvarez, M. M.; Murthy, S.; Vezmar, I.; Wang, Z. L.; Stephens, P. W.; Cleveland, C. L.; Luedtke, W. D.; Landman, U. Nanocrystal Gold Molecules. *Adv. Mater.* **1996**, *8*, 428–433.
- Hostetler, M. J.; Stokes, J. J.; Murray, R. W. Infrared Spectroscopy of Three-Dimensional Self-Assembled Monolayers: N-Alkanethiolate Monolayers on Gold Cluster Compounds. *Langmuir* **1996**, *12*, 3604–3612.
- Alvarez, M. M.; Khoury, J. T.; Schaaff, T. G.; Shafigullin, M. N.; Vezmar, I.; Whetten, R. L. Optical Absorption Spectra of Nanocrystal Gold Molecules. *J. Phys. Chem. B* **1997**, *101*, 3706–3712.
- Schaaff, T. G.; Shafigullin, M. N.; Khoury, J. T.; Vezmar, I.; Whetten, R. L.; Cullen, W. G.; First, P. N.; Gutierrez-Wing, C.; Ascensio, J.; Jose-Yacamán, M. J. Isolation of Smaller Nanocrystal Au Molecules: Robust Quantum Effects in Optical Spectra. *J. Phys. Chem. B* **1997**, *101*, 7885–7891.
- Negishi, Y.; Nobusada, K.; Tsukuda, T. Glutathione-Protected Gold Clusters Revisited: Bridging the Gap between Gold(I)-Thiolate Complexes and Thiolate-Protected Gold Nanocrystals. *J. Am. Chem. Soc.* **2005**, *127*, 5261–5270.
- Donkers, R. L.; Lee, D.; Murray, R. W. Synthesis and Isolation of the Molecule-like Cluster Au₃₈(PhCH₂CH₂S)₂₄. *Langmuir* **2004**, *20*, 1945–1952.
- Zhu, M.; Aikens, C. M.; Hollander, F. J.; Schatz, G. C.; Jin, R. Correlating the Crystal Structure of A Thiol-Protected Au₂₅

- Cluster and Optical Properties. *J. Am. Chem. Soc.* **2008**, *130*, 5883–5885.
- (29) Zhu, M.; Eckenhoff, W. T.; Pintauer, T.; Jin, R. Conversion of Anionic $[\text{Au}_{25}(\text{SCH}_2\text{CH}_2\text{Ph})_{18}]^-$ Cluster to Charge Neutral Cluster via Air Oxidation. *J. Phys. Chem. C* **2008**, *112*, 14221–14224.
- (30) Wu, Z.; Suhan, J.; Jin, R. One-Pot Synthesis of Atomically Monodisperse, Thiol-Functionalized Au_{25} Nanoclusters. *J. Mater. Chem.* **2009**, *19*, 622–626.
- (31) Schaaff, T. G.; Knight, G.; Shafigullin, M. N.; Borkman, R. F.; Whetten, R. L. Isolation and Selected Properties of a 10.4 kDa Gold: Glutathione Cluster Compound. *J. Phys. Chem. B* **1998**, *102*, 10643–10646.
- (32) Dharmaratne, A. C.; Krick, T.; Dass, A. Nanocluster Size Evolution Studied by Mass Spectrometry in Room Temperature $\text{Au}_{25}(\text{SR})_{18}$ Synthesis. *J. Am. Chem. Soc.* **2009**, *131*, 13604–13605.
- (33) MacDonald, M. A.; Zhang, P.; Qian, H.; Jin, R. Site-Specific and Size-Dependent Bonding of Compositionally Precise Gold–Thiolate Nanoparticles from X-ray Spectroscopy. *J. Phys. Chem. Lett.* **2010**, *1*, 1821–1825.
- (34) Zhu, Y.; Qian, H.; Zhu, M.; Jin, R. Thiolate-Protected Au_n Nanoclusters as Catalysts for Selective Oxidation and Hydrogenation Processes. *Adv. Mater.* **2010**, *22*, 1915–1920.
- (35) Negishi, Y.; Takasugi, Y.; Sato, S.; Yao, H.; Kimura, K.; Tsukuda, T. Magic-Numbered Au_n Clusters Protected by Glutathione Monolayers ($n = 18, 21, 25, 28, 32, 39$): Isolation and Spectroscopic Characterization. *J. Am. Chem. Soc.* **2004**, *126*, 6518–6519.
- (36) Shichibu, Y.; Negishi, Y.; Tsunoyama, H.; Kanehara, M.; Teranishi, T.; Tsukuda, T. Extremely High Stability of Glutathione-Protected Au_{25} Clusters Against Core Etching. *Small* **2007**, *3*, 835–839.
- (37) Habeeb Muhammed, M. A.; Shaw, A. K.; Pal, S. K.; Pradeep, T. Quantum Clusters of Gold Exhibiting FRET. *J. Phys. Chem. C* **2008**, *112*, 14324–14330.
- (38) Schaaff, T. G.; Whetten, R. L. Controlled Etching of Au:SR Cluster Compounds. *J. Phys. Chem. B* **1999**, *103*, 9394–9396.
- (39) Toikkanen, O.; Ruiz, V.; Ronholm, G.; Kalkkinen, N.; Liljeroth, P.; Quinn, B. M. Synthesis and Stability of Monolayer-Protected Au_{38} Clusters. *J. Am. Chem. Soc.* **2008**, *130*, 11049–11055.
- (40) Chaki, N. K.; Negishi, Y.; Tsunoyama, H.; Shichibu, Y.; Tsukuda, T. Ubiquitous 8 and 29 kDa Gold:Alkanethiolate Cluster Compounds: Mass-Spectrometric Determination of Molecular Formulas and Structural Implications. *J. Am. Chem. Soc.* **2008**, *130*, 8608–8610.
- (41) Qian, H.; Zhu, M.; Andersen, U. N.; Jin, R. Facile, Large-Scale Synthesis of Dodecanethiol-Stabilized Au_{38} Clusters. *J. Phys. Chem. A* **2009**, *113*, 4281–4284.
- (42) Qian, H.; Zhu, Y.; Jin, R. Size-Focusing Synthesis, Optical and Electrochemical Properties of Monodisperse $\text{Au}_{38}-(\text{SC}_2\text{H}_4\text{Ph})_{24}$ Nanoclusters. *ACS Nano* **2009**, *3*, 3795–3803.
- (43) Qian, H.; Eckenhoff, W. T.; Zhu, Y.; Pintauer, T.; Jin, R. Total Structure Determination of Thiolate-Protected Au_{38} Nanoparticles. *J. Am. Chem. Soc.* **2010**, *132*, 8280–8281.
- (44) Schaaff, T. G.; Shafigullin, M. N.; Khoury, J. T.; Vezmar, I.; Whetten, R. L. Properties of a Ubiquitous 29 kDa Au:SR Cluster Compound. *J. Phys. Chem. B* **2001**, *105*, 8785–8796.
- (45) Hicks, J. F.; Templeton, A. C.; Chen, S.; Sheran, K. M.; Jasti, R.; Murray, R. W.; Debord, J.; Schaaff, T. G.; Whetten, R. L. The Monolayer Thickness Dependence of Quantized Double-Layer Capacitances of Monolayer-Protected Gold Clusters. *Anal. Chem.* **1999**, *71*, 3703–3711.
- (46) Lopez-Acevedo, O.; Akola, J.; Whetten, R. L.; Gronbeck, H.; Hakkinen, H. Structure and Bonding in the Ubiquitous Icosahedral Metallic Gold Cluster $\text{Au}_{144}(\text{SR})_{60}$. *J. Phys. Chem. C* **2009**, *113*, 5035–5038.
- (47) Qian, H.; Jin, R. Controlling Nanoparticles with Atomic Precision: The Case of $\text{Au}_{144}(\text{SCH}_2\text{CH}_2\text{Ph})_{60}$. *Nano Lett.* **2009**, *9*, 4083–4087.
- (48) Fields-Zinna, C. A.; Sardar, R.; Beasley, C. A.; Murray, R. W. Electrospray Ionization Mass Spectrometry of Intrinsically Cationized Nanoparticles, $[\text{Au}_{144/146}(\text{SC}_{11}\text{H}_{22}\text{N}(\text{CH}_2\text{CH}_3)^{3+})_x(\text{S}(\text{CH}_2)_5\text{CH}_3)_y]^{x+}$. *J. Am. Chem. Soc.* **2009**, *131*, 16266–16271.
- (49) Kim, J.; Lerna, K.; Ukaigwe, M.; Lee, D. *Langmuir* **2007**, *23*, 7853–7858.
- (50) Negishi, Y.; Kurashige, W.; Niihori, Y.; Iwasa, T.; Nobusada, K. Isolation, Structure, And Stability of a Dodecanethiolate-Protected $\text{Pd}_1\text{Au}_{24}$ Cluster. *Phys. Chem. Chem. Phys.* **2010**, *12*, 6219–6225.
- (51) Wu, Z.; Lanni, E.; Chen, W.; Bier, M. E.; Ly, D.; Jin, R. High Yield, Large Scale Synthesis of Thiolate-Protected Ag_7 Clusters. *J. Am. Chem. Soc.* **2009**, *131*, 16672–16674.
- (52) Jadzinsky, P. D.; Calero, G.; Ackerson, C. J.; Bushnell, D. A.; Kornberg, R. D. Structure of A Thiol Monolayer-Protected Gold Nanoparticle at 1.1 Ångstrom Resolution. *Science* **2007**, *318*, 430–433.
- (53) Tang, Z.; Xu, B.; Wu, B.; Germann, M. W.; Wang, G. Synthesis and Structural Determination of Multidentate 2,3-Dithiol-Stabilized Au Clusters. *J. Am. Chem. Soc.* **2010**, *132*, 3367–3374.
- (54) Harkness, K. M.; Fenn, L. S.; Cliffel, D. E.; McLean, J. A. Surface Fragmentation of Complexes from Thiolate Protected Gold Nanoparticles by Ion Mobility-Mass Spectrometry. *Anal. Chem.* **2010**, *82*, 3061–3066.
- (55) Zhang, Y.; Shuang, S.; Dong, C.; Lo, C. K.; Paa, M. C.; Choi, M. M. F. Application of HPLC and MALDI-TOF MS for Studying As-Synthesized Ligand-Protected Gold Nanoclusters Products. *Anal. Chem.* **2009**, *81*, 1676–1685.
- (56) Mondloch, J. E.; Wang, Q.; Frenkel, A. I.; Finke, R. G. Development Plus Kinetic and Mechanistic Studies of a Prototype Supported-Nanoparticle Heterogeneous Catalyst Formation System in Contact with Solution: $\text{Ir}(1,5\text{-COD})\text{Cl}/\gamma\text{-Al}_2\text{O}_3$ and Its Reduction by H_2 to $\text{Ir}(0)_n/\gamma\text{-Al}_2\text{O}_3$. *J. Am. Chem. Soc.* **2010**, *132*, 9701–9714.